

# ELECTRICAL BREAKDOWN OF METALLIC SURFACES\*

Mahzad BastaniNejad, Abdelmageed Elmustafa, (ODU, Norfolk, VA)

Mohammad Alsharo'a, Charles M. Ankenbrandt, Pierrick Hanlet, Rolland P. Johnson<sup>#</sup>,

Moyses Kuchnir, Michael Neubauer, David Newsham, Richard Sah, (Muons, Inc., Batavia, IL),

Alfred Moretti, Milorad Popovic, Alvin Tollestrup, Katsuya Yonehara, (Fermilab, Batavia, IL),

Daniel M. Kaplan, (IIT, Chicago, IL) Derun Li, John Byrd, (LBNL, Berkeley CA)

D. V. Rose, C. Thoma, D. R. Welch, (Voss Scientific, LLC, Albuquerque, NM)

## Abstract

An 805 MHz test cell that was originally designed to study the use of RF cavities pressurized with dense hydrogen gas for ionization cooling of muon beams has been used to study the electrical breakdown mechanisms of metallic surfaces. In these studies, the dense hydrogen gas absorbs dark currents and eliminates multipacting, which can complicate the understanding of breakdown in evacuated RF cavities. The measured distributions of the remnants of sparks on the surfaces of the test cell electrodes show that the breakdown probability depends strongly on electrical field in a way that is expected from Fowler-Nordheim field emission. These data and that the maximum sustainable RF gradient increases with the melting temperature of the Cu, Be, Mo, and W electrodes argue for a simple model of electrical breakdown. Namely, any source of field emission on a metallic surface exposed to an electric field will cause a large current to flow through the metal under the source. Ohmic heating will then cause the metal temperature to increase, leading to increased resistance, more heating, and a runaway situation. As its strength is reduced as the metal heats, surface distortions may exacerbate the electron emission. Finally, the metal boils and vaporized metal in the gap effectively shorts the cavity out. Conditioning of the surface occurs as the emission sources (e.g. dust, asperities, inclusions, or regions of low work function) are destroyed by heat or are physically dislodged from the surface.

## INTRODUCTION

The RF breakdown of dense hydrogen gas between metallic electrodes has been studied as part of a program to develop gas-filled RF cavities to be used for muon ionization cooling [1]. A pressurized 805 MHz test cell was used at Fermilab to measure the increase in the breakdown threshold as a function of gas density. The breakdown behavior of copper, molybdenum, and beryllium electrodes as functions of hydrogen gas density have been reported previously as were measurements of RF breakdown using molybdenum electrodes in dense hydrogen in a strong external magnetic field [2].

Scanning electron microscope (SEM) and high resolution optical images of the surfaces of the metallic electrodes used in the experiments were then analyzed to investigate the mechanism of RF breakdown. The images showed evidence for melting and boiling in small regions of ~10 to 20 micron diameter on the molybdenum and beryllium electrode surfaces, suggesting that the vaporized metal might be involved in the breakdown. To further investigate this possibility additional data using tungsten electrodes were taken and are reported here.

In these experiments, the dense hydrogen gas in the cavity prevents electrons or ions to be accelerated to high enough energy to participate in the breakdown process. The gas may absorb much of the energy of the breakdown spark such that the evidence for the cause of the event may not be completely destroyed by the discharge.

The maximum surface gradient of the pressurized cavity is the same as that of a well-conditioned evacuated cavity operating with the same RF parameters using copper components [3]. However, it remains to be proved that the ultimate breakdown mechanisms, when only the fields and metallic surfaces are involved, are the same for pressurized and evacuated cavities.

## APPARATUS

The Test Cell (TC) is a cylindrical RF cavity used for testing in the MuCool Test Area (MTA) at the Fermi National Accelerator Laboratory (Fermilab). The TC is made of copper-plated stainless steel, and has inner height by diameter dimensions of 3.2 x 9.0 in<sup>2</sup>. Within the TC, two 1 inch radius hemispherical electrodes of different materials are interchangeable and mounted along the cylindrical axis as shown in Fig.1. The cavity is powered at  $805 \pm 5$  MHz RF by a klystron located in the Fermilab Linac gallery via an 87 m waveguide and short coaxial line. This RF power is capacitively coupled to the cavity by an epoxy-sealed pressure barrier 23 inches from the TC. A capacitively coupled pickup (PU) probe is mounted in the upper plate of the TC to measure the RF voltage as shown in Figure 1. In addition to the pickup probe, there are two sets of directional couplers (DC) along the coaxial line which are used to measure the transmitted and reflected power into and from the cavity.

---

\* Supported by DOE STTR grants DE-FG02-02ER86145, 05ER86252, 07ER86350, and 07ER86352  
<sup>#</sup> rol@muonsinc.com

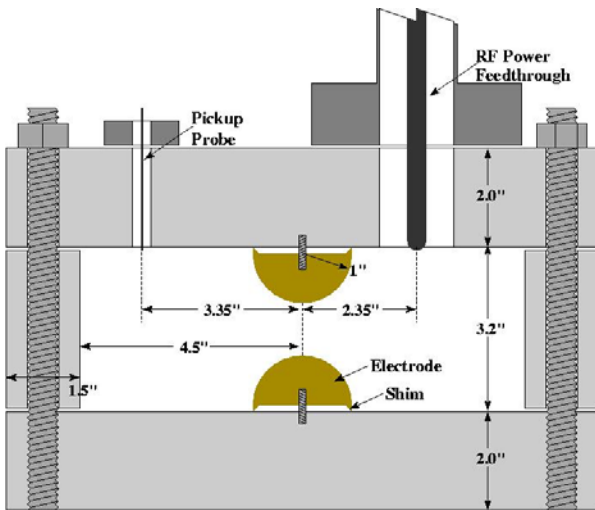


Fig. 1: Cross sectional view of the Muons, Inc. test cell showing replaceable 1" radius Cu, Be, Mo, or W hemispherical electrodes inside a Cu-plated stainless steel pillbox shaped cavity. Pickup and RF power probes are shown, but not the gas input/exhaust port.

Figure 2 is a picture of the TC in the MTA next to the LBNL superconducting solenoid used for the data shown in Figure 3. The data were taken with 100 microsecond pulses at 5 Hz.

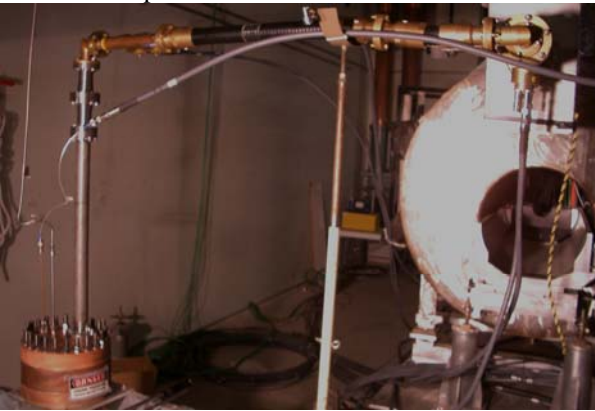


Fig. 2: Picture of the Test Cell in the MTA next to the LBNL superconducting solenoid.

The results for both the external magnetic field on and off are shown in Figure 3. The lower-density region in which the maximum stable gradient rises linearly with absolute pressure is referred to as the Paschen region. The usual model for this is that increased gas density reduces the mean free collision path for ions or electrons so they have less chance to accelerate to energies sufficient to initiate showers. Within errors, the measurements in the Paschen region seem independent of electrode material or on the magnetic field.

As shown in Figure 3, the copper and beryllium electrodes operated stably with surface gradients near 50 MV/m while molybdenum achieved values near 65 MV/m. These results differ considerably from the predictions of most models of breakdown in evacuated cavities [4], which usually include multipacting.

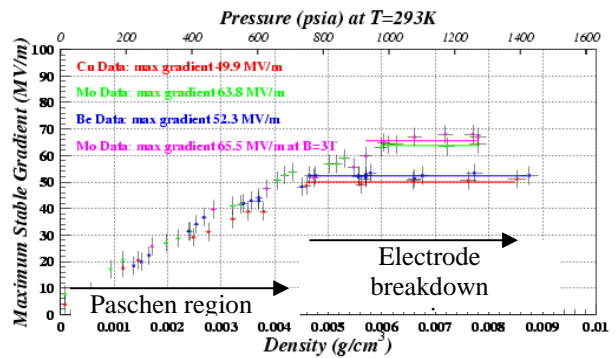


Fig. 3: Measurements of the maximum stable TC gradient as a function of hydrogen gas pressure at 805 MHz with no magnetic field for three different electrode materials: Cu(red), Mo(green), and Be(blue). The cavity was also operated at the same gradients in a 3T field with Mo electrodes(magenta). **W to be added!**

At higher gradients, the electrode metal breaks down. We have studied four electrode materials in order to find the best material for muon cooling applications and to test some theories of RF breakdown. Copper is the standard for RF cavities; molybdenum is a hard material and is expected to have good resistance to breakdown; and beryllium is a low-Z material which might be useful for ionization cooling of muon beams. Tungsten is notable for having very high melting and boiling points. As noted in earlier reports, conditioning of the TC was accomplished within 3 hours, with no evidence of multipacting. However, due to the limited experimental time, we cannot be certain that the maximum gradients achieved could not have been pushed higher with more conditioning time.

## BERYLLIUM SEM ANALYSIS

After the measurements shown in figure 3 were made, the electrodes were examined using a SEM. The surface features of the beryllium and molybdenum electrodes are much easier to distinguish than those on the copper surface. On the Mo and Be electrodes, the regions of high surface gradient in the middle of the gap show similar 10 to 20 micron diameter features that are not seen in the regions of low gradient and therefore we associate them with breakdown events.

Figure 4 shows an area of the Be surface where at least four breakdown events are seen to have occurred. In many cases, there are tadpole-shaped breakdown remnants with a head and tail. On closer examination as seen in figure 5, the head shows evidence of more severe melting and boiling with larger bubble holes than the tail. The assumptions in this interpretation include a belief that the holes are the remains of bubbles because they are round and they look remarkably like bubble remnants in thick cooking sauces. That the tail precedes the head formation is suggested by the melting pattern, where the edge of the

melting region of the head seems to be on top of the tail.



Fig. 4: SEM image of typical breakdown remnants found in the high gradient region of a beryllium electrode. The scale is shown in the lower right corner of this and the following figures.

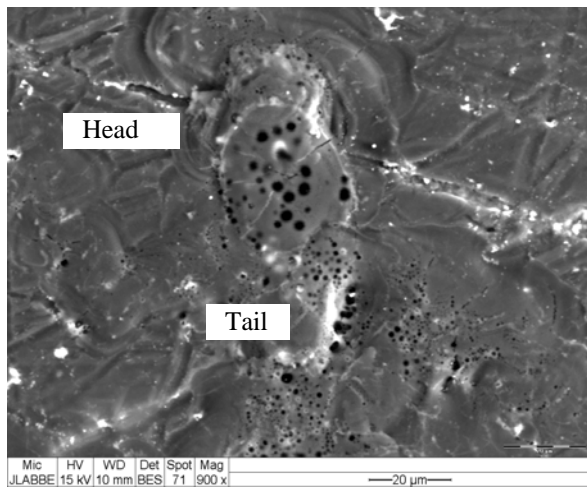


Fig. 5: SEM image of one of the Be tadpole heads, where the transition to the tail region with smaller bubble holes is seen.

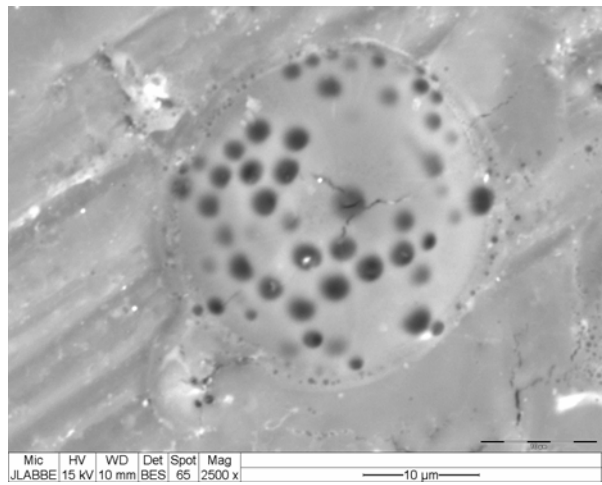


Fig. 6: Closer view of an SEM image of a tadpole head showing the round bubble holes, where the central one has cracks and a vent which may have been formed as the melted region solidified.

### MOLYBDENUM SEM ANALYSIS

The Mo surface features that are unique to the high gradient regions of the electrode do not have tails, but have multiple almost concentric circular melting regions. These melted regions do have holes that are not as circular as in the Be case, but are consistent with the view that the breakdown may be initiated by metallic vapor that emanates from these melting and boiling areas. A possible explanation for the multiple overlapping melting regions is that several conditioning events were needed to destroy the breakdown source.

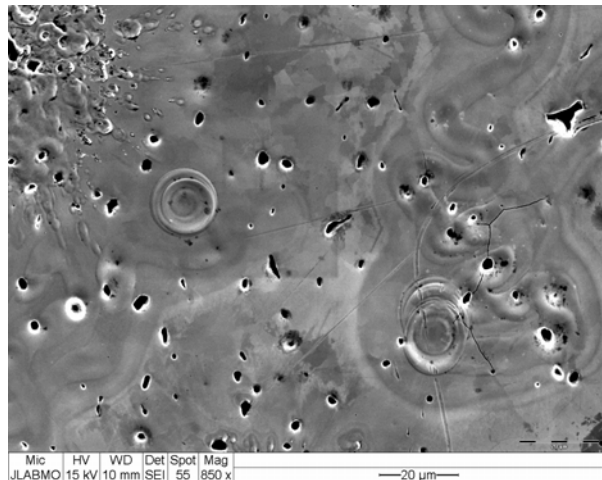


Fig. 7: SEM image of the Mo electrode surface.

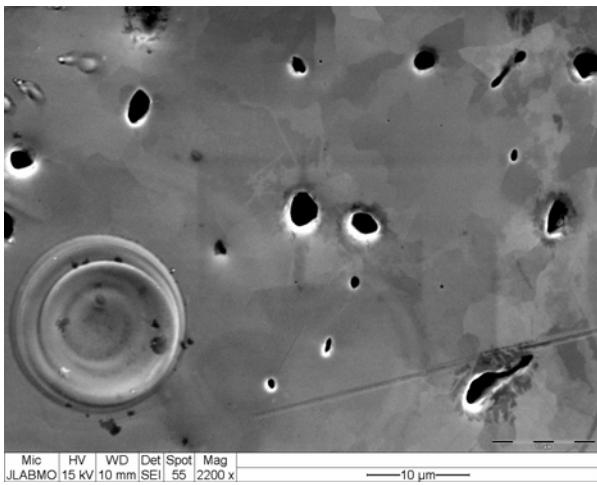


Fig. 8: Closer view of the Mo surface showing concentric rings.

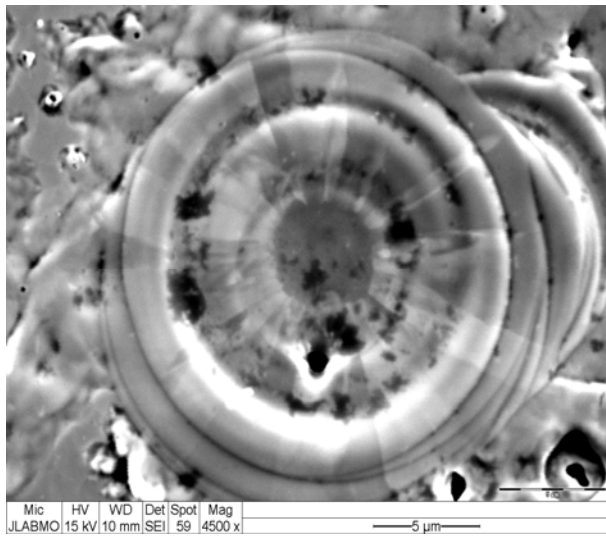


Fig. 9: Close up of one of the Mo concentric melting regions showing vents.

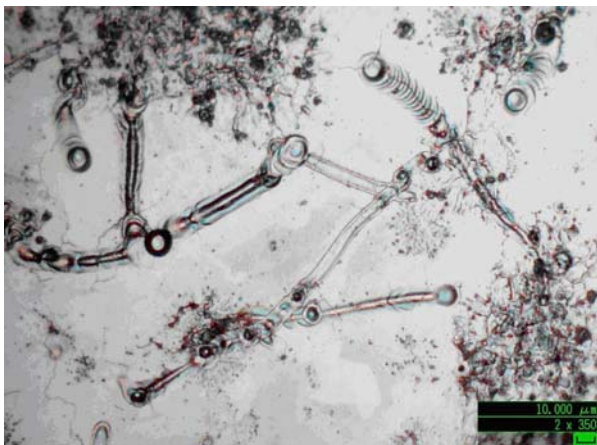


Fig. 10: The W electrodes show two types of breakdown remnants, examples of which are shown in the next two figures.



Fig. 11: A series of apparently melted regions are seen with cracks on the W electrode. Similar cracks do not appear on regions of the electrode that were not exposed to high voltages, indicating the cracks were consequences of the breakdown.

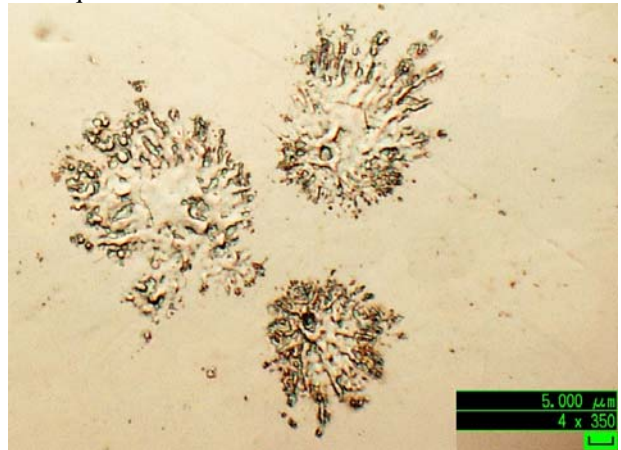


Fig. 12: Some explosive remnants on the W electrode. Here 5 micron diameter craters are surrounded by metallic debris

### EXPERIMENTAL DATA ANALYSIS

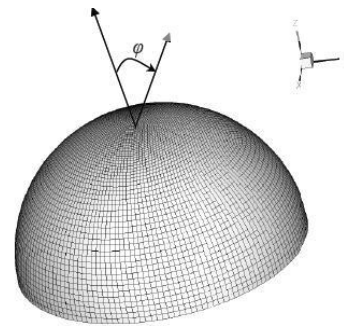


Fig. 13: Definition of the zenith angle  $\varphi$ .

To investigate the correlation of breakdown and the electric field, the local surface density of breakdown remnants as measured with the SEM and optical images has been compared with the maximum expected electric field using an ANSYS model as a function of the zenith angle defined in figure 13. Least squares fits of the data to a power of the predicted maximum electric gradient at the surfaces of the electrodes show good agreement for high values of the exponent. Figure 14 shows the predicted maximum surface gradient (dashed), the data (black with error bars) as described above, and the best least squares fit (red) to the data versus zenith angle for Be. Figures 15 and 16 show the experimental data, the ANSYS model data, and best fits for Mo and W respectively.

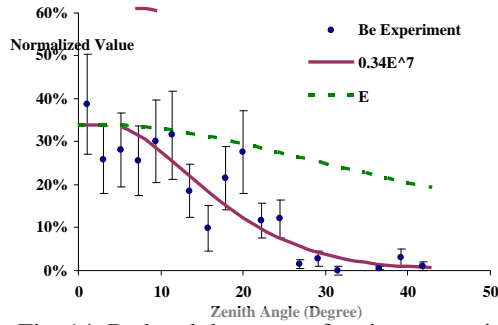


Fig. 14: Be breakdown area fraction vs. zenith angle.

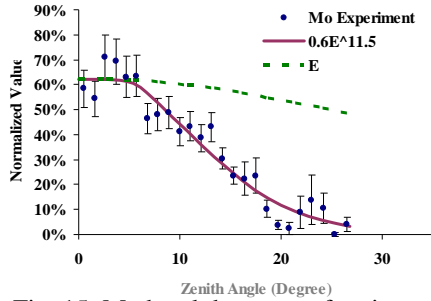


Fig. 15: Mo breakdown area fraction vs. zenith angle.

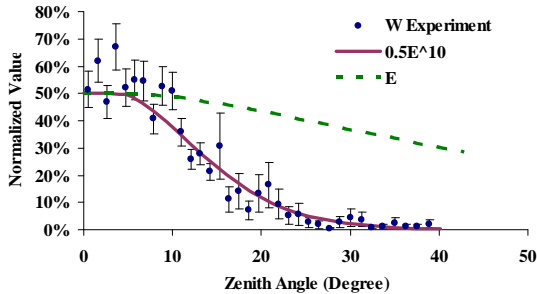


Fig. 16: W breakdown area fraction vs. zenith angle.

For a limited range of electric field, the exponential dependence of emission from a cold cathode derived by Fowler and Nordheim can also be described by a power law. Their theory of field emission due to tunneling of electrons through a barrier in the presence of a high

electric field is based on a quantum mechanical solution to the Schroedinger equation [5]. This theory, which describes field emission measurements over many orders of magnitude [6], can be expressed as:

$$I(E) = \frac{A_{FN}(\beta E)^2}{\varphi} \exp\left(-\frac{B_{FN}\varphi^{3/2}}{\beta E}\right), \quad (1)$$

where  $I$  is the dark current in  $A/m^2$ ,  $E$  is the surface electric field in  $MV/m$ ,  $\varphi$  is the work function of the material in  $eV$ ,

$$A_{FN} = 1.54 \times 10^6 eVA / (MV)^2$$

$B_{FN} = 6830MV / m(eV)^{3/2}$  and  $\beta$  is the ratio of local electric field to the average surface field, which is usually considered a measure of the roughness of the material. Note that  $\varphi$  and  $\beta$  are the only parameters of the theory.

### MELTING OR BOILING POINTS

The maximum stable gradient for each of the four electrode materials is shown on figure 17. For these data, the 805 MHz TC was operated at 5 Hz repetition rate with 100 microsecond long pulses. Either melting or boiling point show a correlation with the maximum gradient that was achieved.

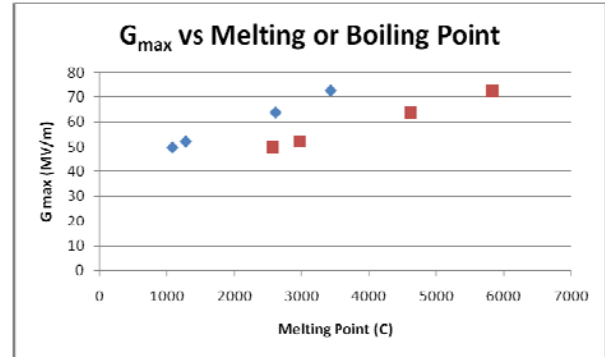


Fig. 17: Maximum stable gradient as a function of metallic melting point (blue diamonds) or boiling point (red squares). From left to right, the four data points correspond to Cu, Be, Mo, and W.

Metal	Cu	Be	Mo	W
Melting point [C]	1083	1278	2617	3422
Boiling Point [C]	2567	2970	4612	5828
Heat of fusion [J/mm <sup>3</sup> ]	1.8		3.4	3.7
Heat of vaporization [J/mm <sup>3</sup> ]	42		63	87

Table I: Material properties

### SIMPLE MODEL OF BREAKDOWN

The correlation of maximum gradient with melting and boiling points, the SEM and optical pictures, and the Fowler-Nordheim dependence on the observed breakdown probability argue for a simple breakdown

model that should apply to pressurized RF cavities as well as vacuum cavities for any frequency, including DC.

1. There should be some source (e.g. bump, inclusion, grain boundary,...) which by some combination of roughness and work function parameters generates a strong Fowler-Nordheim field emission current.

2. The electrons that are emitted must come from somewhere. They must flow through the metal below the source and the current density should be very high next to the source.

3. Ohm's law should apply and  $I^2 R$  with  $R$  being a strong function of temperature should create a runaway temperature. In the case of a W light-bulb filament the voltage limits the current. In the case of F-N there is no current limitation, although the source of electrons must lead to some limitations.

4. a. The melting point of a metal is related to the bond strength. When it gets hot enough, the metal can deform to produce more or enhanced peaks with larger local fields and even more local current. This may be the situation that Jim Norem et al. [7] have modeled, where peaks can be blown off and vaporized.

b. Or the metal can just boil to vent vapor into the gap. The pictures of our Be electrodes show this behavior.

c. Or more explosive boiling could actually expel some of the melted metal. Perhaps some of the molten copper balls found in vacuum cavities after breakdown are from the initiation of breakdown as described above rather than as a consequence of the spark that followed. (I have been inspired by seeing how far blobs of spaghetti sauce can go while the sauce simmers). We see this behavior in some of the W data.

## DISCUSSION

The data described here represent ex post facto observations and certain aspects of them are not known. For example, it is not known whether the surface features of the electrodes as shown in figures 4 through 12 have any information about the initiation of the breakdown event or if they are simply consequences of the breakdown spark.

## REFERENCES

- [1] R. P. Johnson et al., proceedings of LINAC2004, <http://bel.gsi.de/linac2004/PAPERS/TU203.PDF>
- [2] P. Hanlet et al., EPAC06
- [3] Moretti et al. (~50MV/m, 20 to 100 us pulses at 5 Hz)
- [4] Perry Wilson, Theoretical Prediction for the ..., <http://www.slac.stanford.edu/grp/ara/HGWorkshop/TH EORY%20OF%20RF%20BREAKDOWN.pdf>

The volume of a 10 micron diameter cylinder with a 15 micron depth (corresponding to the electromagnetic skin depth) is  $V \sim 25 \pi \times 15 \sim 1000$  cubic microns, or  $1000/(10,000)^3 = 10^{-(3-12)} = 10^{-9}$  cm<sup>3</sup> or  $10^{-6}$  mm<sup>3</sup>. An ANSYS model of the TC shows that the amount of stored energy in the TC when the surface gradient is near 50 MV/m at the tip of the electrode is approximately 1 Joule. This is to be compared with the  $15 \times 10^{-6}$  J required to melt the volume of tungsten in question as shown in Table I. Namely, most of the stored energy has gone somewhere other than into the remnants that are observed. Is it possible, for example, that the gas could absorb the stored energy?

Analytic [8] and Monte Carlo [9] models of showers produced by beams of ionizing radiation in the hydrogen-filled TC indicate that electrons and ions can survive for relatively long times while they are caught in the oscillating RF field. Since the electrons are light enough that they actually can move and impart energy to surrounding gas molecules, they are expected to reduce the quality factor of the cavity. (Experiments to add electronegative dopants such as SF<sub>6</sub> and CO<sub>2</sub> to the hydrogen gas in order to mitigate this effect are being designed.)

If it is the case that most of the stored energy in the high-pressure TC is absorbed by the gas during RF breakdown, there are some interesting consequences:

- 1) the remnant analyses that lead to the rather simple picture of breakdown as due to Ohmic heating of metal beneath an emitting source are more likely to be true,
- 2) The technique to condition cavities to be used for vacuum operation by using dense gases may depend on the electron survival time in the gas,
- 3) Adding dopants to mitigate the long electron survival time in hydrogen gas will imply that much more damage will occur to the electrodes during conditioning. This test can be made quickly.

The detuning of the cavity that causes the quick reflection of power that we see after a breakdown may be a hint for another mechanism to get rid of the stored energy before it destroys the remnant. Namely, the stored energy can leave the same way it came in, through the coax feed. We should be able to model that.

- 
- [5] R. H. Fowler and L. Nordheim, "Electron emission in intense electric fields," in Proc. Roy. Soc. (London), A119, pp. 173–181, 1928.
  - [6] W. P. Dyke and J. K. Trolan, "Field emission: Large current densities, space charge, and the vacuum arc," Phys. Rev., 89, pp. 799–808, 1953.
  - [7] J. Norem et al.
  - [8] Tollestrup note
  - [9] Dave Rose note